

Stochastic scalar mixing models accounting for turbulent frequency multiscale fluctuations

Olivier Soulard ^a, Vladimir Sabel'nikov ^{a,*}, Michael Gorokhovski ^b

^a ONERA, DEFA/IEFCA, Chemin de la Hunière, 91761 Palaiseau Cedex, France

^b CNRS, CORIA UMR 6614, Université de Rouen, 76821 Mont-Saint-Aignan, France

Received 8 January 2004; accepted 27 March 2004

Abstract

Two new scalar micromixing models accounting for a turbulent frequency scale distribution are investigated. These models were derived by Sabel'nikov and Gorokhovski [Second International Symposium on Turbulence and Shear FLOW Phenomena, Royal Institute of technology (KTH), Stockholm, Sweden, June 27–29, 2001] using a multiscale extension of the classical interaction by exchange with the mean (IEM) and Langevin models. They are, respectively, called Extended IEM (EIEM) and Extended Langevin (ELM) models.

The EIEM and ELM models are tested against DNS results in the case of the decay of a homogeneous scalar field in homogeneous turbulence. This comparison leads to a reformulation of the law governing the mixing frequency distribution. Finally, the asymptotic behaviour of the modeled PDF is discussed.

© 2004 Published by Elsevier Inc.

Keywords: Micromixing; Turbulent reactive flow; Probability density functions

1. Introduction

Over the past twenty years, the probability density function (PDF) approach has become a common and powerful tool for modeling turbulent reactive flows (Pope, 1985). One of its main advantages is that no model is required for the chemical source term appearing in the reactive scalar equations. However, the process of molecular mixing cannot be represented by the one-point information carried by a PDF: a scalar micromixing model is thus necessary to account for this phenomenon.

If molecular mixing takes place at the smallest diffusive scales of the turbulent spectrum, its intensity roughly depends on the local values of the scalar dissipation frequency, which in turn depend on the scalar structures created by turbulence. As a consequence, micromixing models not only have to account for a small scale phenomenon—molecular mixing—but also for its interaction with a fully turbulent spectrum, from

large convective scales down to the smallest diffusive scales.

Modeling this interaction still remains a challenging problem. Actually, most scalar mixing models used in practical calculations do not account for it. For instance, the interaction by exchange with the mean (IEM) model (Villermaux and Devillon, 1972), also known as LMSE (Dopazo and O'Brien, 1974), or the Langevin model (Pope, 1985) are based on a single mean time scale. Other models have been proposed (Fox, 1995, 1997) in order to correct this approximation, but at the price of a non-negligible increase in complexity.

In this article, two new scalar mixing models accounting for the influence of a turbulent frequency scale repartition while keeping a simple formulation are investigated. These models were derived by Sabel'nikov and Gorokhovski (2001) from the IEM and Langevin models and are named, respectively, Extended IEM (EIEM) and Extended Langevin Model (ELM). They are evaluated in the case of the decay of a homogeneous scalar in homogeneous turbulence and the results are compared against the DNS data of Eswaran and Pope (1988). This investigation leads to the reformulation of

* Corresponding author. Fax: +33-69-93-61-82.

E-mail address: vladimir.sabelnikov@onera.fr (V. Sabel'nikov).

Nomenclature

c	scalar concentration	β	modified log-normal law function
$c' = c - \langle c \rangle$	scalar fluctuation	Re_λ	Taylor scale Reynolds number
ω_c	scalar frequency	$s = (c - \langle c \rangle)/\sigma$	non-dimensionalized scalar
ε_c	scalar dissipation	$\xi = \ln c' $	logarithm of scalar fluctuations
σ	scalar rms value	$\gamma = (\xi - \langle \xi \rangle)/\sigma_\xi$	reduced scalar
σ_M	maximum value of σ	f_c	PDF of c
σ_0	initial value of σ	$f_{c\chi}$	joint PDF of c and χ
κ	scalar molecular diffusion coefficient	d_0	Langevin model constant
ω	modeled scalar frequency	S_4	flatness factor
$\chi = \ln(\omega/\langle \omega \rangle)$	logarithm of the scalar frequency	S_6	hyperflatness factor
Ω	EIEM model function	$W(t)$	Standard Wiener process
m_1, m_2, C_χ	log-normal law constants	$\langle \cdot \rangle$	mean value
T	log-normal law time scale	$\langle \cdot \cdot \rangle$	conditional mean value
α	modified log-normal law constant		

the law governing the frequency fluctuations. The asymptotic behaviour of the new models is also examined.

2. Derivation of the Extended IEM and Extended Langevin models

In this section, following Sabel'nikov and Gorokhovski (2001), a method for modeling the effects of a turbulent time scale distribution on scalar mixing is described and applied to derive two new models from the classical IEM and Langevin models. All the subsequent derivations are made for homogeneous scalars in homogeneous turbulence.

2.1. Extended IEM model

The IEM model is most easily introduced in a Lagrangian framework: alongside a fluid particle trajectory, the scalar concentration evolves according to the deterministic relaxation law:

$$dc = -\langle \omega_c \rangle (c - \langle c \rangle) dt \quad (1)$$

with c the concentration of the scalar, $\omega_c = \varepsilon_c/\sigma^2$ the scalar frequency, $\varepsilon_c = \kappa |\nabla c|^2$ the scalar dissipation and $\sigma^2 = \langle c^2 \rangle - \langle c \rangle^2$ the scalar variance. Mean quantities are denoted by angle brackets. The scalar concentration of the fluid particle is thus driven towards the mean concentration at a speed proportional to the mean scalar frequency. Beyond its simplicity and efficiency, a striking feature of the IEM model is that it describes mixing in terms of mean—and not local—values. As a consequence, the IEM model can only describe mixing in a global way, as only one type of scalar structure is represented: those defined by the mean scalar fre-

quency. In contrast, turbulent mixing involves a whole spectrum of structure sizes ranging from thin zones, with high scalar dissipation and strong mixing, to larger zones with weaker mixing and scalar gradients. These zones are distributed highly non-uniformly in space and time. A notable consequence of this defect is that the IEM model will not relax the shape of the PDF for the decay of a homogeneous scalar in homogeneous turbulence.

In order to correct this insufficiency, Sabel'nikov and Gorokhovski (2001) proposed replacing the single frequency scale $\langle \omega_c \rangle$ by a stochastic intermittent process ω . As a result, fluid particles will possess their own frequency and behave as if belonging to different structures. A whole distribution of scales is thus represented.

The main difficulty now amounts to devising a model for ω . As a first approximation, a log-normal evolution can be chosen. Such a law allows one to represent a statistically stationary transfer between the scales of a developed turbulent spectrum and is usually used to model the turbulent velocity dissipation frequency (Pope and Chen, 1990).

The EIEM model (Sabel'nikov and Gorokhovski, 2001) is then defined by the following stochastic equations:

$$\begin{cases} dc = -\Omega \omega (c - \langle c | \omega \rangle) dt \\ d\chi = -(\chi - m_1) dt/T + \sqrt{2m_2/T} dW(t), \\ \chi = \ln(\omega/\langle \omega \rangle) \end{cases} \quad (2)$$

with $W(t)$ a standard Wiener process, $m_1 = \langle \chi \rangle$ and $m_2 = \langle (\chi - \langle \chi \rangle)^2 \rangle$ the mean and variance of the quantity χ and T the log-normal law time scale.

The mean scalar value conditioned on the frequency $\langle c | \omega \rangle$ replaces in Eq. (2) the mean scalar value $\langle c \rangle$ used in the IEM model (1). This substitution has been

introduced in order to conserve the scalar mean during the mixing process.

Ω is a function set in order to preserve a decrease of the variance σ^2 coherent with the exact equation in homogeneous turbulence:

$$\frac{d\sigma^2}{dt} = -2\langle \varepsilon_c \rangle = -2\langle \omega_c \rangle \sigma^2 \quad (3)$$

By multiplying the first equation of system (2) by $2c$, one obtains the evolution of the variance for the EIEM model. Then, identification with Eq. (3) yields:

$$\Omega = \frac{\langle \omega_c \rangle \sigma^2}{\langle \omega (\langle c^2 | \omega \rangle - \langle c | \omega \rangle^2) \rangle} \quad (4)$$

The log-normal law constants are chosen according to the DNS results of Yeung and Pope (1989). This study suggests the following Reynolds number dependence for m_2 in the range $38 \leq Re_\lambda \leq 93$:

$$m_2 = 0.29 \ln Re_\lambda - 0.36 \quad (5)$$

where Re_λ is the Reynolds number based on the Taylor scale. Besides, from the relation $\langle e^\chi \rangle = 1$, the following equality is deduced:

$$m_1 = -(1/2)m_2 \quad (6)$$

As for the log-normal law time scale, it is defined by $T^{-1} = C_\chi \langle \omega \rangle$ where $C_\chi = 1.6$ is a constant.

From system (2) and using standard techniques (Gardiner, 1985), it is possible to deduce the equation of the joint PDF $f_{c\chi}$ of c and χ :

$$\begin{aligned} \frac{\partial f_{c\chi}}{\partial t} = & \frac{\partial}{\partial c} [\Omega \langle \omega \rangle e^\chi (c - \langle c | \chi \rangle) f_{c\chi}] + \frac{\partial}{\partial \chi} [C_\chi \langle \omega \rangle (\chi - m_1) f_{c\chi}] \\ & + \frac{\partial^2}{\partial \chi^2} [C_\chi \langle \omega \rangle m_2 f_{c\chi}] \end{aligned} \quad (7)$$

As a consequence of its definition, the EIEM model incorporates the effects of a distribution of time scales in a turbulent flow. Further history is also accounted for as mixing will depend on the evolution of the frequency from initial time up to the time considered.

2.2. Extended Langevin model

The IEM model is deterministic and generates a perfect correlation alongside the trajectories in phase space. The idea of the Langevin model is to introduce some de-correlation by adding a random source in the scalar equation. As defined by Sabel'nikov and Gorokhovski (2001), the Langevin model is given by

$$\begin{cases} dc = -a \langle \omega_c \rangle (c - \langle c \rangle) dt + \sqrt{2b \langle \omega_c \rangle c(1-c)} dW \\ a = 1 + d_0 \frac{\langle c(1-c) \rangle}{\sigma_M^2} \\ b = d_0 \frac{\sigma^2}{\sigma_M^2} \end{cases} \quad (8)$$

where the same notations as before are being used. σ_M^2 is the maximum value of the scalar variance: $\sigma_M^2 =$

$\langle c \rangle (1 - \langle c \rangle)$ and d_0 is a constant controlling the rate of PDF relaxation. In particular, for $d_0 = 0$, the EIEM model is recovered. The variance equation can be deduced from Eq. (8) and is shown not to depend on d_0 . What is more, the identification of this equation with the Eq. (3) yields a definition for Ω identical to the one obtained from the EIEM model in Eq. (4).

The scalar concentration must be constrained to vary between 0 and 1. Boundedness is achieved through the limiting function $c(1-c)$ as a factor of the noise term. It has to be noted that this limiting function, while simple to devise for a single scalar problem, can become complex for a multiscalar case.

As with the IEM model, the Langevin model is based on a single time scale. Thus, it is possible to apply a procedure similar to the one used with the IEM model to create the EIEM model, which leads to the following formulation for the ELM stochastic model (Sabel'nikov and Gorokhovski, 2001):

$$\begin{cases} dc = -a \Omega \omega (c - \langle c | \omega \rangle) dt + \sqrt{2b \Omega \omega c(1-c)} dW \\ a = 1 + d_0 / \sigma_M^2 \langle c(1-c) | \omega \rangle \\ b = d_0 / \sigma_M^2 (\langle c^2 | \omega \rangle - \langle c | \omega \rangle^2) \end{cases} \quad (9)$$

The equation for the joint PDF $f_{c\chi}$ of c and χ is given in homogeneous turbulence by

$$\begin{aligned} \frac{\partial f_{c\chi}}{\partial t} = & \frac{\partial}{\partial c} [a \Omega \langle \omega \rangle e^\chi (c - \langle c | \chi \rangle) f_{c\chi}] \\ & + \frac{\partial^2}{\partial c^2} [b \Omega \langle \omega \rangle e^\chi c(1-c) f_{c\chi}] + \frac{\partial}{\partial \chi} [C_\chi \langle \omega \rangle (\chi - m_1) f_{c\chi}] \\ & + \frac{\partial^2}{\partial \chi^2} [C_\chi \langle \omega \rangle m_2 f_{c\chi}] \end{aligned} \quad (10)$$

The previous remarks made about the EIEM model also apply to the ELM model. In Section 3, as a first guess, a value $d_0 = 1$ is chosen. In the future, a study should be undertaken to further understand the influence of d_0 on the results.

3. Scalar mixing in homogeneous turbulence

The PDF Eqs. (7) and (10) derived from the EIEM and ELM models have been numerically solved in the case of the decay of a homogeneous passive scalar field in homogeneous turbulence. A second-order finite-volume method based on an essentially non-oscillatory (ENO) interpolation was used. The initial conditions as well as the evolution of the mean scalar dissipation were taken from Eswaran and Pope (1988).

3.1. Comparison of the models with Eswaran and Pope (1988) DNS data

Fig. 1 compares the PDF evolutions obtained with the EIEM and ELM models with Eswaran and Pope's

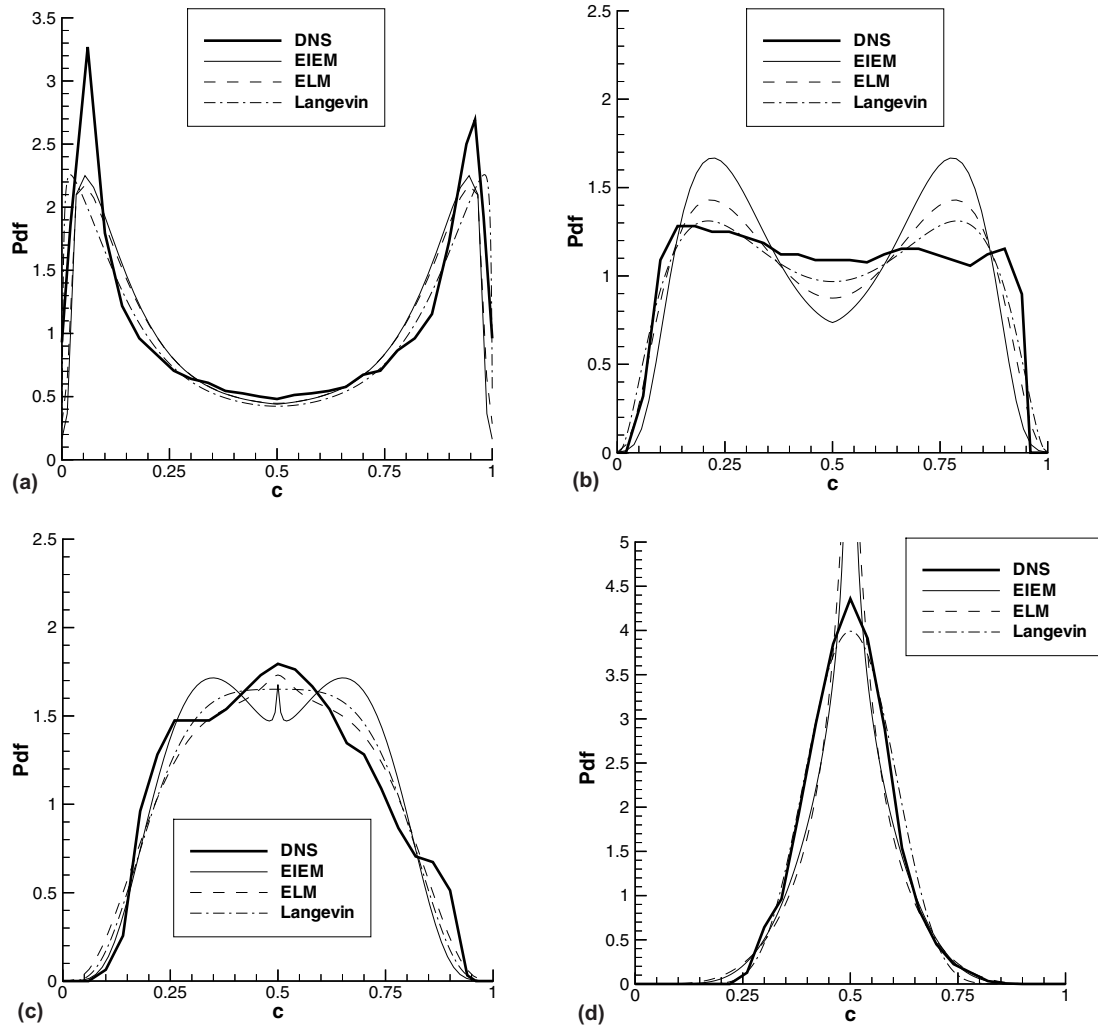


Fig. 1. Comparison of modeled scalar PDFs against DNS data. The log-normal law is used. $(\langle\omega\rangle t, \sigma/\sigma_0) = (0.22, 0.99)$ (a); $(1.49, 0.73)$ (b); $(2.11, 0.55)$ (c); $(3.47, 0.27)$ (d).

DNS calculations. The case considered corresponds to the values $k_s/k_0 = 1$ and $Re_\lambda = 50$ in Eswaran and Pope (1988). (k_s is the mean wave number in the “top-hat distribution of the initial scalar field and k_0 is the lowest non-zero wave number indicated by the geometrical scale.)

The main result is the good agreement found between modeled PDFs and PDFs from DNS. Both models, starting from an initial double peak, yield transient shapes which are qualitatively similar to those obtained with DNS. Characteristic shapes such as a flat almost uniform distribution, a dome-like PDF or a bell shaped PDF are indeed successively observed in both cases. This agreement is also observed in Fig. 2 for the flatness factor $S_4 = \langle c'^4 \rangle / \sigma^4$ and hyperflatness factor $S_6 = \langle c'^6 \rangle / \sigma^6$.

Differences are nonetheless observed: both models exhibit a strong super-Gaussian PDF, as the values of S_4 and S_6 rapidly become greater than the flatness and

hyperflatness values obtained with a Gaussian distribution: $S_4^{\text{Gauss.}} = 3$ and $S_6^{\text{Gauss.}} = 15$. This tendency is much stronger than the one observed with DNS. More importantly, for the EIEM model, the initial double peak influences for a longer time the shape of the PDF, and a very acute central peak is formed at larger times. In order to correct this defect, a modification of the log-normal law is proposed.

3.2. Modified log-normal law

For the EIEM model, the evolution of the PDF shape is entirely due to the intermittent time scale spectrum; this suggests the inadequacy of using a log-normal law to represent the behaviour of a mean scalar frequency in homogeneous turbulence. Indeed, as already mentioned, the log-normal law allows the representation of the statistically stationary transfer between the scales of a developed turbulent spectrum. However, during the

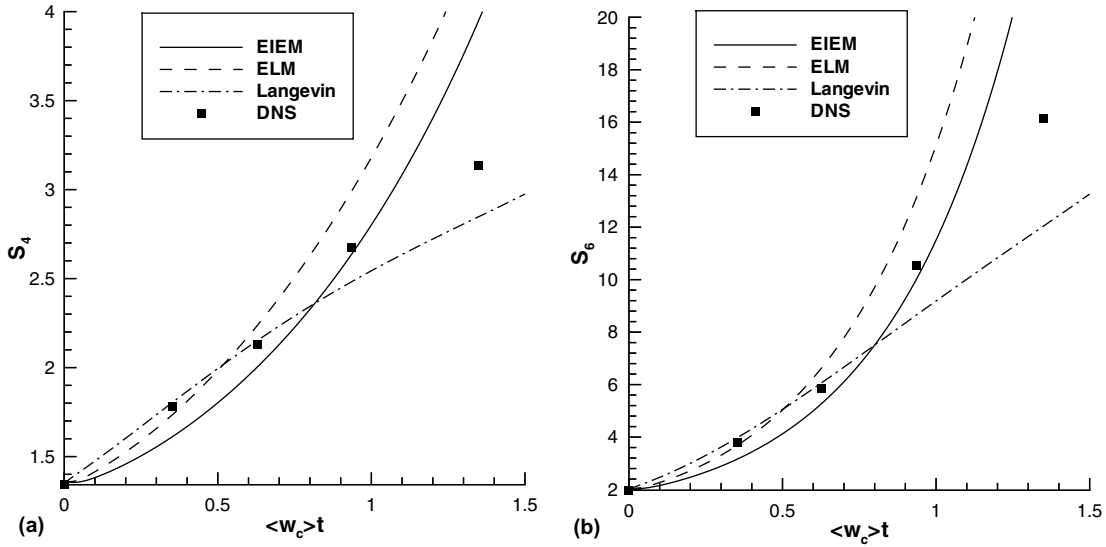


Fig. 2. Comparison of flatnesses and hyperflatnesses against DNS data. The log-normal law is used. Flatness (a); hyperflatness (b).

mixing of a scalar in homogeneous turbulence, transfer between scalar scales is strong at the beginning of the process as large structures are broken or stirred into smaller ones but becomes weaker at larger times, as the mixture becomes more and more homogeneous. This phenomenon is not accounted for by the log-normal law. The following frequency law is thus proposed in order to represent it

$$\omega = \langle \omega \rangle \beta \exp \left[\alpha \frac{\sigma}{\sigma_M} \chi \right] \quad (11)$$

where $\alpha = 1.25$ is a constant chosen to best fit the data and β is a function introduced in order to ensure that the mean values of the right- and left-hand sides of Eq. (11) are equal:

$$\beta = \exp \left[\alpha \frac{\sigma}{2\sigma_M} \left(2m_1 + \alpha \frac{\sigma}{\sigma_M} m_2 \right) \right] \quad (12)$$

As the mixing gets more advanced, the variance σ decreases so that the fluctuations of the frequency become weaker and eventually vanish. In this limit, the classical IEM and Langevin models are recovered.

New calculations were conducted using this modified law, with all parameters kept constant in regards to the previous results. Fig. 3 shows a global improvement of the PDF evolutions, and, in particular, the absence of a strong peak at the times considered. It is also observed (see Fig. 4) that S_4 and S_6 do not increase exponentially any longer and exhibit mostly sub-Gaussian features for the interval of time considered ($S_4 < S_4^{\text{Gauss.}}$ and $S_6 < S_6^{\text{Gauss.}}$).

3.3. Asymptotic behaviour

The issue discussed in this paragraph is the existence of a self-similar behaviour at large times for the modeled

PDFs. In other words, the question addressed here is: is it possible to find a rescaling of the scalar field for which the form of the PDF remains invariant?

3.3.1. Formulation based on the log-normal law

Self-similar solutions are first sought as stationary solutions for the PDF of the non-dimensionalized scalar $s = (c - \langle c \rangle) / \sigma$. Analysis shows that such a solution could be reached for the ELM model, but not for the EIEM models. Fig. 5(a) shows the asymptotic PDF obtained with the ELM model and the non-stationary shape of the PDF obtained with the EIEM model at some large time $\langle \omega_c \rangle t = 20$.

Both solutions exhibit a strong central peak as well as exponential-like tails. Such non-Gaussian PDFs have been observed in several experimental and numerical studies (Shraiman and Siggia, 1994; Chaves et al., 2001; Jaber et al., 1996). For the EIEM and ELM models, the exponential-like tails result from the influence of low frequencies. From a Lagrangian point of view, they arise from fluid particles having followed a weak mixing path due to the configuration of the turbulent frequency field. On the other hand, the peak is due to high frequencies and to particles having followed strong mixing paths. For the EIEM model, the peak is over-estimated.

For the EIEM model, a rescaling of the scalar field yielding a self-similar PDF can be obtained from the following line of argument: one can notice that Eq. (2) is similar in form to the equation governing the evolution of an infinitesimal line element (Batchelor, 1952), except for the noise which is supposed to be Gaussian for the line element case. This suggests using some of the results and rescalings indicated in works related to line element deformation (Batchelor, 1952; Girimaji and Pope, 1989).

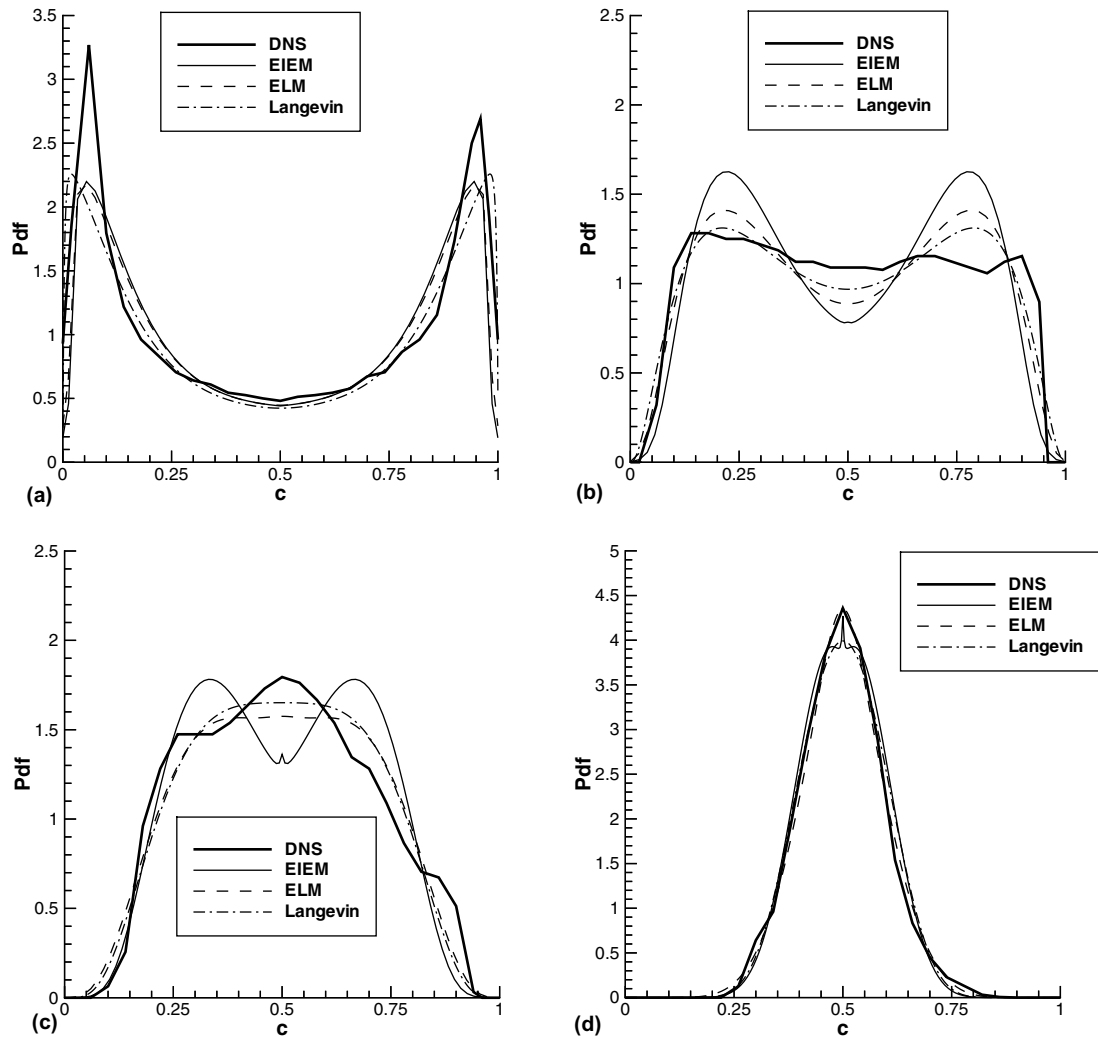


Fig. 3. Comparison of modeled scalar PDFs against DNS data. The modified law (Eq. (11)) is used. $(\langle \omega \rangle t, \sigma/\sigma_0) = (0.22, 0.99)$ (a); $(1.49, 0.73)$ (b); $(2.11, 0.55)$ (c); $(3.47, 0.27)$ (d).

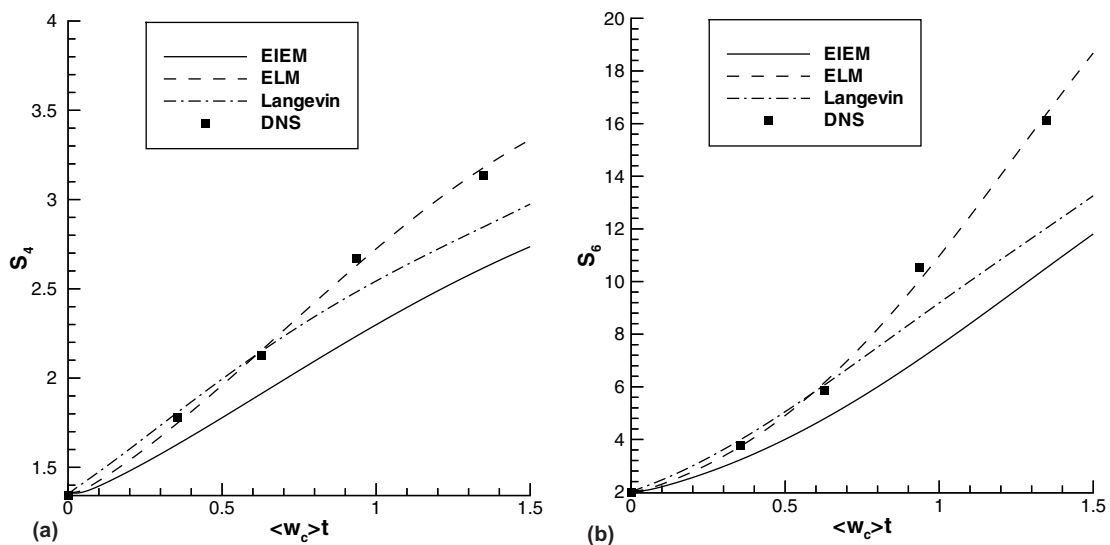


Fig. 4. Comparison of flatnesses and hyperflatnesses against DNS data. The modified law (11) is used. Flatness (a); hyperflatness (b).

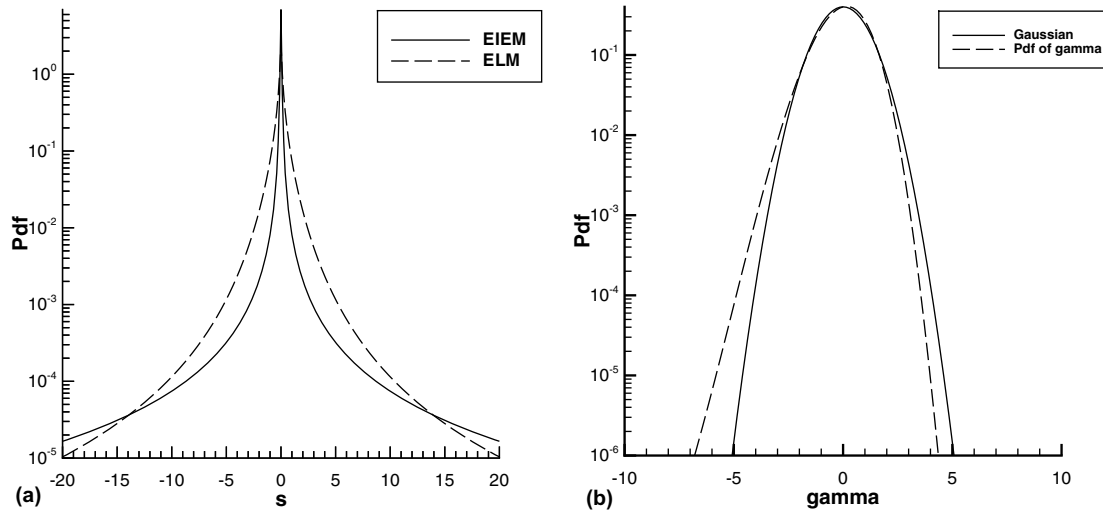


Fig. 5. Self-similar solutions for the EIEM and ELM models based on a log-normal law. (a) Stationary solution for the PDF of s for the ELM model and solution obtained at $\langle \omega_c \rangle t = 20$ for the EIEM model. (b) Stationary solution for the PDF of the reduced scalar γ for the EIEM model.

Let us assume for simplicity that Ω is constant equal to unity and that c has a symmetric PDF. It is also supposed that, at $t = 0$, the relation $\langle c|\omega \rangle = \langle c \rangle$ is true so that it remains valid for all times (see Sabel'nikov and Gorokhovski, 2001, for this last condition). Then, one obtains for the variable $\xi = \ln |c'|$ the following evolution equation:

$$\frac{d\xi}{dt} = -\omega, \quad \xi = \ln |c'| \quad (13)$$

Now, Eq. (13) is similar to Taylor's diffusion equation (Tennekes and Lumley, 1972), with ω a non-Gaussian stationary process. Thus, Eq. (13) will yield stationary statistics for the reduced scalar (see Girimaji and Pope, 1989 where mathematically similar problems are analyzed):

$$\gamma = \frac{\xi - \langle \xi \rangle}{\sigma_\xi} \quad (14)$$

where σ_ξ is the rms value of ξ .

The PDF of γ is then solved numerically. The numerical procedure used in this case requires great care, as the PDFs of γ exhibit long tails which carry information about the initial solution and are slow to converge. Moreover, interaction between these tails and the domain boundaries can generate significant numerical errors. Despite these difficulties, keeping in mind their potential influence on the validity of the solution, a stationary PDF of γ was obtained as shown on Fig. 5(b). This self-similar solution for the EIEM model is negatively skewed, indicating a strong predominance of small $|c|$ values.

3.3.2. Formulation based on the modified law (Eq. (11))

The formulation of the EIEM and ELM models based on the modified frequency law (Eq. (11)) naturally

leads to the existence of stationary solutions for the PDF of the reduced scalar s : as the variance vanishes ($\sigma/\sigma_M \rightarrow 0$), ω tends to a constant equal to its mean $\langle \omega \rangle$ so that the EIEM and ELM models tend to their classical counterpart, the IEM and Langevin models, respectively. As the IEM model gives an invariant standardized PDF for s and the Langevin model admits a Gaussian asymptotic PDF, stationary solutions are eventually reached for the EIEM and ELM models.

Fig. 6(a) shows the asymptotic solutions obtained numerically starting from a double peak initial solution. A stationary solution was obtained for both models for times on the order of $\langle \omega_c \rangle t = 20$. The EIEM model still delivers a PDF with exponential like tails, but far less flat than with the log-normal law. As for the ELM model, a Gaussian PDF is indeed obtained. This last feature shows that the ELM model has the ability to qualitatively reproduce the results described in Jaber et al. (1996). The ELM actually produces transient non-Gaussian PDFs and an asymptotic Gaussian solution (see Fig. 4).

It should be noted that the asymptotic solution reached by the EIEM model depends on the initial solution. Fig. 6(b) shows the stationary PDFs obtained for different initialisations. Stationary solutions were also obtained for times on the order of $\langle \omega_c \rangle t = 20$. The differences can be explained as follows: starting from an initial double peak solution, the two peaks first have to be amalgamated into a single peak and, from there, exponential tails can start to appear. Meanwhile, $\sigma \rightarrow 0$ so that the formation of the peak and exponential tails is progressively slowed down. When starting from an initial Gaussian solution, the exponential tails are stretched from the beginning of the mixing process and the peak is enhanced. Consequently, when $\sigma \rightarrow 0$, larger tails and a larger peak are observed compared with the initial

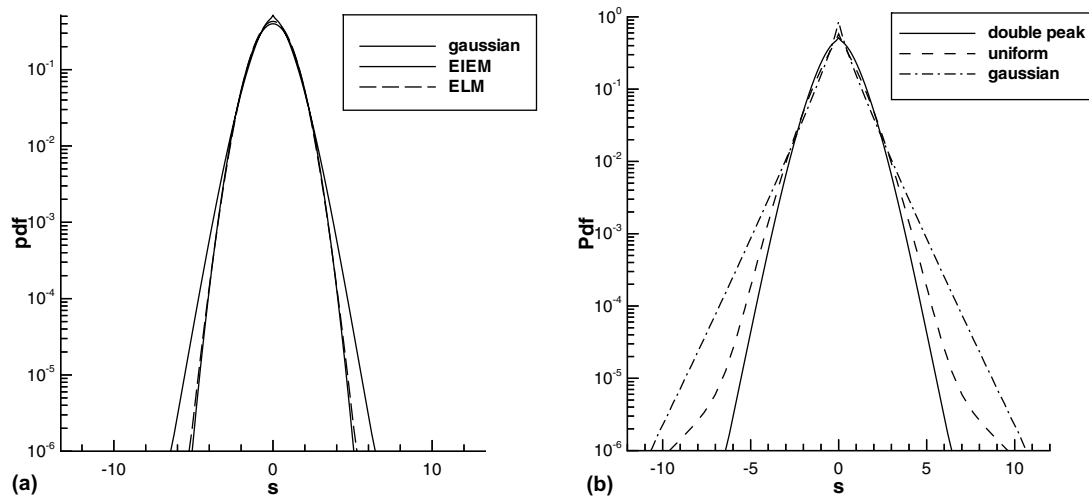


Fig. 6. Self-similar solutions for the EIEM and ELM models based on the modified law (Eq. (11)). (a) Stationary solution for the PDF of s for the ELM and EIEM model starting from an initial double-peak. (b) Stationary solutions obtained with the EIEM model starting from various initial conditions (double-peak, uniform distribution, Gaussian distribution).

double peak case. The uniform distribution appears as an intermediate case between the double peak and the Gaussian initialisations. Despite those differences, the observed PDFs still possess some common features such as exponential tails and a strong central peak. As for the ELM model, a Gaussian asymptotic solution is obtained whatever the initial condition.

4. Conclusion

Two new scalar mixing models, the Extended IEM and Extended Langevin models, have been examined. Both models account for the influence of a fully turbulent time-scale spectrum while keeping a simple formulation. This last feature makes the models attractive for industrial applications.

Both yield a qualitatively good agreement with DNS calculations for intermediate decay times and in particular do not have the main shortcoming of the standard IEM model of no evolution of the initial shape of the PDF alongside the scalar fluctuation decay process.

A first formulation of the models based on a frequency described by a log-normal law was used. Some limits of this law have been pointed out and a new formulation based on a modified log-normal law has been proposed.

For all models, exponential-like tails at large intermediate times are observed due to selective events of weak scalar decay at low mixing frequency. This behaviour is preserved in the long-time limit for the EIEM and ELM models based on the log-normal law, as well as for the EIEM based on the modified law. For the ELM model based on the modified law, a Gaussian PDF is obtained. Both types of behaviour are consistent

with recent discussions on the mixing of randomly advected scalars.

References

- Batchelor, G.K., 1952. The effect of homogeneous turbulence on material lines and surfaces. *Proc. Royal Soc. A* 213, 349–366.
- Chaves, M., Eyink, G., Frish, U., Vergassola, M., 2001. Universal decay of scalar turbulence. *Phys. Rev. Lett.* 86 (11), 2305–2308.
- Dopazo, C., O'Brien, E., 1974. An approach to the autoignition of a turbulent mixture. *Acta Astronaut.* 1, 1239–1266.
- Eswaran, V., Pope, S.B., 1988. Direct numerical simulation of the turbulent mixing of a passive scalar. *Phys. Fluids* 31, 506–520.
- Fox, R.O., 1995. The spectral relaxation model of the scalar dissipation rate in homogeneous turbulence. *Phys. Fluids* 7, 1082–1094.
- Fox, R.O., 1997. The lagrangian relaxation model of the scalar dissipation in homogeneous turbulence. *Phys. Fluids* 9, 2364–2386.
- Gardiner, C.W., 1985. *Handbook of Stochastic Methods*, second ed. Springer.
- Girimaji, S.S., Pope, S.B., 1989. Material element deformation in isotropic turbulence. *Fluid Dynamics and Aerodynamics Program*, Cornell University, FDA-89-14.
- Jaberi, F.A., Miller, R.S., Madnia, C.K., Givi, P., 1996. Non-Gaussian scalar statistics in homogeneous turbulence. *J. Fluid Mech.* 313, 241–282.
- Pope, S.B., 1985. PDF methods for turbulent reactive flows. *Prog. Energy Combust. Sci.* 11, 119–192.
- Pope, S.B., Chen, Y.L., 1990. The velocity-dissipation probability density function model for turbulent flows. *Phys. Fluids, A* 2, 1432–1449.
- Sabel'nikov, V.A., Gorokhovski, M., 2001. Extended LMSE and Langevin models of the scalar mixing in the turbulent flow. In: *Second International Symposium on Turbulence and Shear Flow Phenomena*, Royal Institute of technology (KTH), Stockholm, Sweden, June 27–29.
- Shraiman, B.I., Siggia, E.D., 1994. Lagrangian path integrals and fluctuations in random flow. *Phys. Rev. E* 49 (4), 2912–2927.
- Tennekes, H., Lumley, J.L., 1972. *A First Course in Turbulence*. The MIT Press.

Villermaux, J., Devillon, J.C., 1972. Représentation de la redistribution des domaines de ségrégation dans un fluide par un modèle d'interaction phénoménologique. In: 2nd Int. Symp. Chem. React. Engng. Amsterdam, B-1-13.

Yeung, P.K., Pope, S.B., 1989. Lagrangian statistics from direct numerical simulations of isotropic turbulence. *J. Fluid Mech.* 207, 531–586.